

## THE CIRCUMSTELLAR ENVIRONMENT OF MWC297: ISO RESULTS AND FIRST EXPECTATIONS

M. Benedettini<sup>1</sup>, S. Pezzuto<sup>1</sup>, T. Giannini<sup>2</sup>, D. Lorenzetti<sup>2</sup>, B. Nisini<sup>2</sup>, and F. Strafella<sup>3</sup>

<sup>1</sup>CNR-Istituto di Fisica dello Spazio Interplanetario, Area di Ricerca di Roma Tor Vergata, via Fosso del Cavaliere 100, 00133 Roma, Italy

<sup>2</sup>Osservatorio Astronomico di Roma, via Frascati 33, 00040 Monte Porzio, Italy

<sup>3</sup>Dipartimento di Fisica Università di Lecce, 73100 Lecce, Italy

### ABSTRACT

The ISO SWS and LWS full grating spectra of the Herbig Be star MWC297 are presented. The spectra are dominated by a strong continuum; in addition, in the SWS range (2.3-45 $\mu$ m), emission lines from the HI recombination series, PAH emission and absorption by solid CO<sub>2</sub>, H<sub>2</sub>O, and silicates have been observed while in the LWS spectrum (43-197 $\mu$ m) [OI] and [CII] fine structure lines have been detected.

The NIR-FIR data have been combined with ground based photometry to derive the spectral energy distribution (SED) from optical to radio wavelengths. The observed SED has been compared with the SED's computed with a spherical dusty envelope model parametrized by a density and temperature law in order to probe if such a circumstellar matter distribution is compatible with the observations, deriving also suitable values for the spectral type, the extinction and the distance. Consistent determination of the extinction and estimates of both the source mass loss rate and the size of the emitting ionized region have been derived by the analysis of the HI recombination lines of the Brackett, Pfund and Humphreys series observed by ISO together with Paschen and Brackett lines observed from the ground.

The results are somewhat hampered by the large beam size of the ISO instruments. We show how the Photoconductor Array Camera and Spectrometer (spectral range 60 - 210  $\mu$ m) on board the FIRST satellite, with its high spatial resolution (9.4 arcsec) will be able to improve our understanding of the physical conditions in the close neighbourhood of MWC297 and, more generally, to shed light on the distribution of the circumstellar matter around the Herbig Ae/Be stars.

Key words: Stars: individual: MWC297 – Stars: mass-loss – circumstellar matter

### 1. INTRODUCTION

The Herbig Ae/Be (HAEBE) star MWC297 has originally been classified as a B0 pre-Main Sequence star (Bergen et al. 1988) positioned at a distance of 450 pc (Cantò et al. 1984), but Drew et al. (1997) revised this view attributing to this object a spectral type B1.5, a distance

of 250 pc and a later evolutionary state. KAO images by Di Francesco et al. (1998) show the presence of a quite extended circumstellar region, whose size is  $\sim 60'' \times 50''$ , with a total flux of  $1100 \pm 540$  Jy at 50 $\mu$ m and  $1300 \pm 640$  Jy at 100  $\mu$ m.

In this contribution we analyse the NIR-FIR spectra of MWC297, provided by the two spectrometers on board the Infrared Space Observatory (ISO) satellite in order to derive the distribution and the physical parameters of circumstellar matter. However, the large spatial resolution of the ISO spectrometers, in particular at FIR wavelengths ( $\sim 80''$ ), are not good enough to directly resolve the morphology of the circumstellar envelope around HAEBE stars; on the contrary, the higher spatial resolution (9.4 arcsec) of the Photoconductor Array Camera and Spectrometer (PACS, spectral range 60 - 210  $\mu$ m) on board the FIRST satellite, will be suitable for this purpose. We will show the capabilities of the PACS instrument in answering some of the still open questions that we address in our analysis.

### 2. ISO OBSERVATIONS

MWC297 (RA(2000): 18h 27m 39.5s; DEC(2000):  $-3^\circ 49' 52.1''$ ) was observed with the two spectrometers, the Short Wavelength Spectrometer (SWS, de Graauw et al. 1996) and the Long Wavelength Spectrometer (LWS, Clegg et al. 1996), on board ISO, during revolution 708. The spectra (SWS: 2.3-45 $\mu$ m, LWS: 43-197 $\mu$ m) have been carried out with the AOT01 full grating scan mode, corresponding to a resolution from 250 to 600 for SWS and  $\sim 200$  for LWS. Raw data have been processed with the OLP 7 and 9 for SWS and LWS respectively. An additional analysis has been performed in order to remove glitches, average the different spectral scans and remove the fringes present in the LWS long-wavelength range.

The spectra are dominated by a strong continuum with superimposed several emission lines and features both in emission and in absorption (fig. 1 and 2). In particular, in the SWS range we detect 23 emission lines from the Brackett, Pfund and Humphreys HI recombination series, PAH emission at 3.53, 6.22, 13.56 and 14.21  $\mu$ m, silicate broad band absorption at 9.7 and 16.4  $\mu$ m and absorption features at 2.96 and 4.27  $\mu$ m by CO<sub>2</sub> and H<sub>2</sub>O ice respectively. In the LWS spectrum, fine structure lines from [OI]

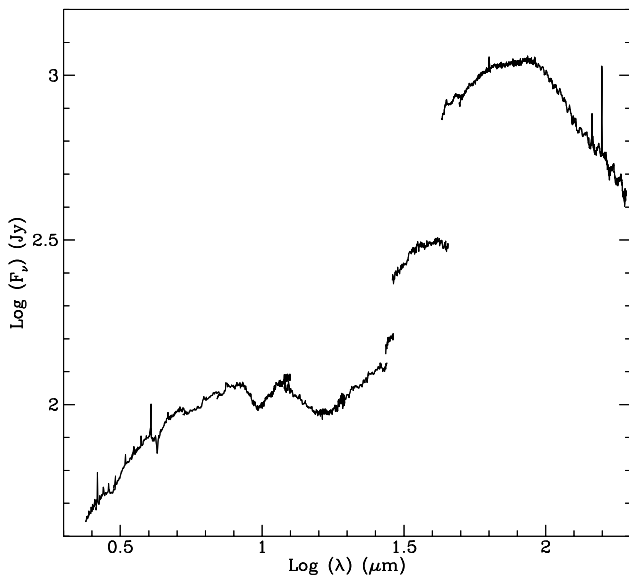


Figure 1. SWS and LWS spectra of MWC297, the single spectra of the 10 LWS detectors have been stitched.

at 63.17 and 145.53  $\mu\text{m}$  plus the [CII] at 157.80  $\mu\text{m}$  have been detected (Lorenzetti et al. 1999).

### 3. CONTINUUM SPECTRUM

From the inspection of fig. 1, beam effects due to the extent of the emitting region are clearly evident since portions of the spectrum observed with different beamsizes do not overlap.

The spectral energy distribution (SED) derived from ISO data and complemented with photometric measurements from optical to radio wavelengths have been compared with a spherical dusty model (see Pezzuto et al. (1997)) for a description of the model and references to photometric data). The temperature and density distributions of the circumstellar envelope are parametrized by a radial power law with index  $q$  and  $p$ , respectively.

By fitting the observed SED (fig. 3), the following parameters have been derived:  $q=0.5$ ,  $p=1.1$ , SpT=B2, distance=280 pc and  $A_V=7.5$  mag. The spectral type and the distance estimates are in agreement with the values given by Drew et al. (1997). We note that in the SWS spectral range the model predicts a flux density higher than the observed value, this can be ascribed to the extendness of the source which is probably larger than the SWS beams as can be inferred from the inspection of the ISO spectra (see fig. 1) in which a sharp rise in the flux density is observed whenever the beam aperture increases (*i.e.* at 27, 29, 45  $\mu\text{m}$ ). Moreover, the SWS beam at 45  $\mu\text{m}$  ( $20'' \times 33''$ ) is smaller than the size of the emitting region at 50

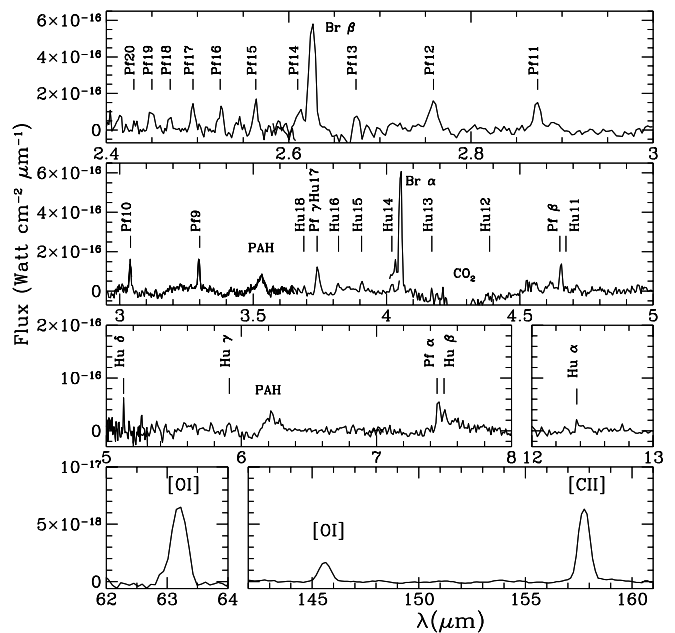


Figure 2. Continuum subtracted parts of SWS and LWS spectra where emission lines have been detected.

$\mu\text{m}$  measured by Di Francesco et al. (1998) ( $(57 \pm 13)'' \times (46 \pm 15)''$ ).

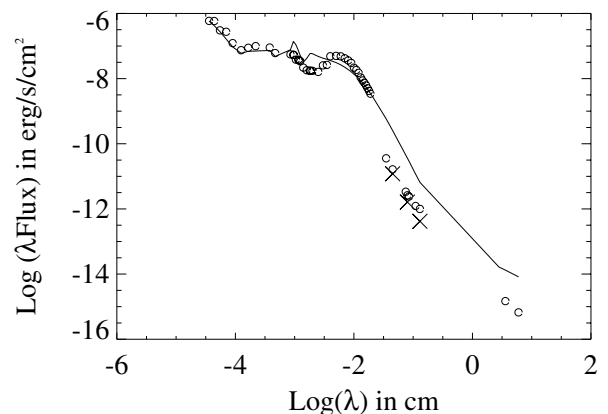


Figure 3. SED of MWC297: circles are photometric data, solid line is the model, crosses are model data after taking into account the beam size (diffraction) at (sub)mm wavelengths.

### 4. HI RECOMBINATION LINES

The observed HI recombination lines have been compared with a wind model (see Benedettini et al. 1998) which considers a spherical gas envelope, fully ionized up to a distance  $R$  from the central star, with a constant rate of mass loss. The gas is assumed to be in LTE condition and

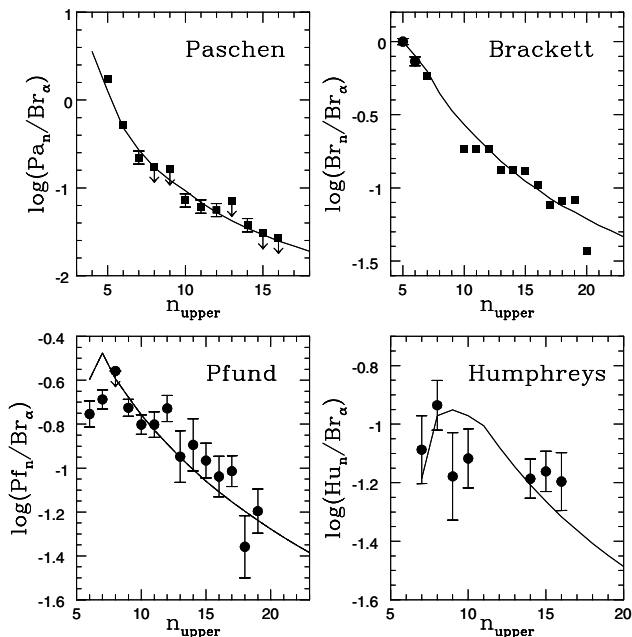


Figure 4. Line ratios of the Paschen, Brackett, Pfund and Humphreys lines with respect to the  $Br_\alpha$  line; circles are the SWS observations while squares are ground based observations. Solid line represents the modeled line ratios corresponding to the best fit parameters:  $\dot{M}=9 \cdot 10^{-7} M_\odot \text{yr}^{-1}$ ,  $R=27r_*$  and  $A_V=7.5 \text{ mag}$ .

to have a constant temperature of  $T=10^4$  K. The adopted gas velocity law is:

$$v(r) = v_i + (v_{max} - v_i)[1 - (r_*/r)] \quad (1)$$

where  $v_i=20 \text{ km s}^{-1}$  is the initial velocity,  $v_{max}=380 \text{ km s}^{-1}$  is the maximum wind velocity (derived from the  $H\alpha$  observed profiles, Finkenzeller & Mundt 1984) and  $r_*=3.2 \cdot 10^{11} \text{ cm}$  is the stellar radius of a B1.5 ZAMS star (Thompson 1984).

We use the Pfund and Humphreys lines observed by ISO to derive the mass loss rate and the dimension of the ionized circumstellar region and the Brackett and Paschen lines observed from the ground by Thompson et al. (1977) and McGregor et al. (1984) to constrain the dust extinction. Assuming the distance of 250 pc and the extinction law by Rieke & Lebofsky (1985), we derive the following best fit parameters:  $\dot{M}=9 \cdot 10^{-7} M_\odot \text{yr}^{-1}$ ;  $R=27r_*$  and  $A_V=7.5 \text{ mag}$  (see fig. 4). We note that the visual extinction estimate is in agreement with the value derived with the previous method and comparable with the value of 8.3 mag given by Hillenbrand et al. (1992).

## 5. THE ANOMALOUS [OI] LINE RATIO

The ratio between the two [OI] lines  $[OI]63\mu\text{m}/[OI]145\mu\text{m} = 1.8 \pm 0.2$  is extremely low with respect to the model predictions of both PDR (Kaufman et al. 1999) and shock (Hollenbach & McKee 1989) which are never smaller than

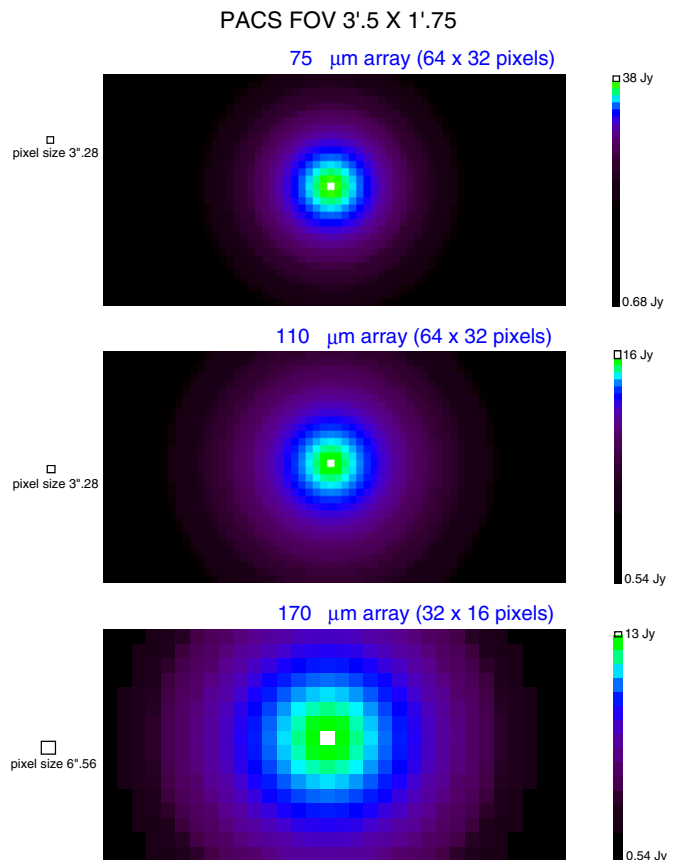


Figure 5. The emission from MWC297 and its extended circumstellar envelope predicted by our model as expected to be imaged by PACS (without taking into account for diffraction). A diffuse background has been added to the synthetic maps adopting the values measured at  $50\mu\text{m}$  and  $100\mu\text{m}$  by Di Francesco et al. (1998) after scaling for the different beamsizes; at  $170\mu\text{m}$  we used the same value measured at  $100\mu\text{m}$ .

10. Ratios smaller than 10 have been found also in other YSOs observed by ISO (Saraceno et al. 1998) but the value measured in MWC297 is the lowest.

Such a ratio could be accounted for if both lines were optically thick and arising from a gas at  $T \sim 80 \text{ K}$ , but this would imply a column density  $N_H \gg 5 \cdot 10^{22} \text{ cm}^{-2}$  contrasting with our determination of  $N_H \sim 1.5 \cdot 10^{22} \text{ cm}^{-2}$ , derived from the  $A_V$  value. Alternatively, the observed ratio could be interpreted as due to strong absorption of the [OI] $63\mu\text{m}$  line by cold ( $\sim 100 \text{ K}$ ) OI present along the line of sight.

## 6. FIRST EXPECTATIONS

The better spatial resolution of PACS (9.4 arcsec) with respect to the ISO spectrometers will be crucial to solve some of the open problems which have been highlighted

above; these considerations can be applicable more generally, to the whole class of HAEBE stars.

1. By using the PACS photometric capability (FOV =  $3.5 \times 1.75$  arcmin<sup>2</sup>) it will be possible to spatially resolve the circumstellar envelope around the HAEBE stars and to derive the physical parameters of the matter distribution. As an example in fig. 5 we show how the extended spherical emission foreseen by our model is expected to be imaged by the PACS arrays at 75, 110 and 170  $\mu$ m.
2. By using the PACS spectroscopic capability a map of  $47'' \times 47''$  in both the 63 $\mu$ m and 145 $\mu$ m [OI] lines can be used to probe their ratio in order to verify if the anomalous value measured by ISO is locally generated in each spatial sample or results from averaged contributions encompassed by the larger ISO sampling.

#### REFERENCES

- Benedettini M., Nisini B., Giannini T. et al., 1998, *A&A* 339, 159
- Bergen Y.K., Kozlov V.P., Krivstov A.A. et al., 1988, *Astrophys. J.* 28, 529
- Cantó J., Rodríguez L.F., Calvet N. et al., 1984, *ApJ* 282, 631
- Clegg P.E., Ade P.A.R., Armand C. et al. 1996, *A&A*, 315, L38
- de Graauw T., Haser L.N., Beintema D.A. et al., 1996 a, *A&A* 315, L49
- Di Francesco J., Evans II N.J., Harvey P.M. et al., 1998, *ApJ* 509, 324
- Drew J.E., Busfield G., Hoare M.G. et al., 1997, *MNRAS* 286, 538
- Finkenzeller U., Mundt R., 1984, *A&AS* 55, 109
- Hollenbach D., McKee C.F., 1989, *ApJ* 342, 306
- Hillenbrand L.A., Strom S.E., Vrba F.J., Keene J., 1992, *ApJ* 397, 613
- Kaufman M.J., Wolfire M.G., Hollenbach D.J., Luhman M., 1999, *ApJ* 527, 795
- Lorenzetti D., Tommasi E., Giannini T. et al., 1999, *A&A* 346, 604
- McGregor P.J., Persson S.E., Cohen J.G., 1984, *ApJ* 286, 609
- Pezzuto S., Strafella F., Lorenzetti D., 1997, *ApJ* 485, 290
- Rieke G.H., Lebofsky M.J., 1985, *ApJ* 288, 618
- Saraceno P., Nisini B., Giannini T. et al., 1998, *APS Conf. Ser.* 132, "Star Formation with the Infrared Space Observatory", pag. 233
- Thompson R.I., Strittmatter P.A., Erickson E.F. et al., 1977, *ApJ* 218, 170
- Thompson R.I., 1984, *ApJ* 283, 165